Free Radical Biology and Medicine 137 (2019) 194–200

Contents lists available at ScienceDirect

Free Radical Biology and Medicine

journal homepage: www.elsevier.com/locate/freeradbiomed

Original article

Hsp22 overexpression induces myocardial hypertrophy, senescence and reduced life span through enhanced oxidative stress

Didier Morin[a,*,1], Romain Long[a,1], Mathieu Panel[a], Lydie Laure[a], Adela Taranu[a], Cindy Gueguen[a], Sandrine Pons[a], Valerio Leoni[b], Claudio Caccia[c], Stephen F. Vatner[d], Dorothy E. Vatner[d], Hongyu Qiu[d], Christophe Depre[d], Alain Berdeaux[a], Bijan Ghaleb[a]

[a] U955-IMRB, Equipe 03, Inserm, UPEC, Ecole Nationale Vétérinaire d'Alfort, Créteil, France
[b] Laboratory Medicine, Desio Hospital, University of Milano Bicocca, Milan, Italy
[c] Laboratory of Clinical Pathology and Medical Genetics, Institute Neurologico IRCCS Carlo Besta, Milano, Italy
[d] Department of Cell Biology and Molecular Medicine, New Jersey Medical School, Rutgers, The State University of New Jersey, USA

Keywords:
Hsp22 overexpression
Oxidative stress
Myocardial hypertrophy
Senescence
Life span

A B S T R A C T

H11 kinase/Hsp22 (Hsp22) is a small heat shock protein, which, when overexpressed cardiac specifically in transgenic (TG) mice, induces stable left ventricular (LV) hypertrophy. Hsp22 also increases oxidative phosphorylation and mitochondrial reactive oxygen species (ROS) production, mechanisms mediating LV hypertrophy, senescence and reduced lifespan. Therefore, we investigated whether ROS production mediates LV hypertrophy, senescence and reduced life span in Hsp22 TG mice. Survival curves revealed that TG mice had a 48% reduction in their mean life span compared to wild type (WT) mice. This was associated with a significant increase in senescence markers, such as p16, p19 mRNA levels as well as the percentage of β-galactosidase positive cells and telomerase activity. Oxidized (GSSG)/reduced (GSH) glutathione ratio, an indicator of oxidative stress, and ROS production from 3 major cellular sources was measured in cardiac tissue. Hearts from TG mice exhibited a decrease in GSH/GSSG ratio together with increased ROS production from all sources. To study the role of ROS, mice were treated with the antioxidant Tempol from weaning to their sacrifice. Chronic Tempol treatment abolished oxidative stress and overproduction of ROS, and reduced myocardial hypertrophy and Akt phosphorylation in TG mice. Tempol also significantly extended life span and prevented aging markers in TG mice. Taken together these results show that overexpression of Hsp22 increases oxidative stress responsible for the induction of hypertrophy and senescence and ultimately reduction in life span.

1. Introduction

The stress-responsive Heat shock protein 22 (Hsp22) is highly expressed in the heart and skeletal muscle [1,2] and is involved in the response to the two most common forms of cardiac cell stress, i.e. pressure overload and hypoxia. Its cardiac expression is increased in various models of cardiac hypertrophy and ischemia, including human patients, underlying a possible participation in the mechanisms of cardiac cell growth and cell survival [3]. It was previously shown that a transgenic (TG) mouse model with cardiac-specific overexpression of Hsp22, reproducing the increased expression found in patients, is characterized by a pattern of chronic and stable myocardial hypertrophy [1,4]. Mitochondrial Hsp22 was also shown to regulate lifespan in *Drosophila* [5].

We also previously showed that Hsp22 increases oxidative phosphorylation [6]. This was associated with an enhancement of the production of mitochondrial reactive oxygen species (ROS; [7]). ROS have emerged as key mediators in cardiac pathophysiology, playing a key role stimulating pathways leading to cardiac hypertrophy [8], senescence and reduced lifespan [9]. Accordingly, the goal of this investigation was to determine whether Hsp22 overexpression reduced longevity and age-related myocardial dysfunction, as well as myocardial hypertrophy through ROS production and oxidative stress. To accomplish these goals, we first compared the life span of wild type

Abbreviations: GSSG, Oxidized glutathione; GSH, reduced glutathione; H2O2, hydrogen peroxide; LV, left ventricular; ROS, reactive oxygen species; TG, transgenic; TSPO, translocator protein; VDAC, voltage-dependent anion channel; WT, wild type

* Corresponding author. INSERM U955-équipe 03, Faculté de Médecine de Créteil, 8 rue du Général Sarrail, 94010, Créteil Cedex, France.
E-mail address: didier.morin@inserm.fr (D. Morin).

[1] Authors share co-first authorship.

https://doi.org/10.1016/j.freeradbiomed.2019.04.035
Received 5 February 2019; Received in revised form 12 April 2019; Accepted 26 April 2019
Available online 29 April 2019
0891-5849/

(WT) and TG mice and characterized their ROS production and oxidative stress. Then we compared these responses after chronic treatment with the whole cell antioxidant, Tempol, which is a superoxide dismutase mimetic agent that has been shown to reduce oxidative stress in mice [10].

2. Methods

All animal procedures used in this study were in strict accordance with the European Community Council Directive 2010/63/EU and recommendations of the French Ministère de l'Agriculture. All experimental procedures were approved by the Animal Ethics Committee Afssa/ENVA/Universite Paris Est Creteil (approval number 09/10/12-5).

2.1. Animal model

We used TG mice (male FVB/NRj) expressing the coding sequence of human Hsp22 and a C-terminal hemagglutinin tag as previously described [2] and their WT littermates. This overexpression of Hsp22 was cardiac-specific. When indicated, mice were treated with the antioxidant 4-hydroxy-2,2,6,6-tetramethylpiperidin-1-oxyl (Tempol, 100 mg/kg, po; [10]) administered daily for 7–9 weeks from the weaning to the day of sacrifice.

Additional WT and TG mice were bred in the same conditions until their death and survival curves were plotted. The mean life span was calculated using Kaplan-Meier analysis. To establish the survival curve with Tempol treatment, mice were fed with Tempol (100 mg/kg/day) or with vehicle (water) during 27 weeks (or until the natural death).

2.2. Isolation of cardiac mitochondria, mitoplasts and outer mitochondrial membranes

Mitochondria were isolated by differential centrifugation as described previously [7]. Left ventricular (LV) tissue was homogenized in a buffer (220 mM mannitol, 70 mM sucrose, 10 mM HEPES, 2 mM ethylene glycol-bis(β-aminoethyl ether)-N,N,N′,N'-tetraacetic acid (EGTA), pH 7.4 at 4 °C) supplemented with 0.25% bovine serum albumin, using a Potter-Elvehjem glass homogenizer in a final volume of 10 ml. The homogenate was filtered through cheese cloth and centrifuged at 1000 g for 5 min at 4 °C. The pellet was discarded and the supernatant was centrifuged at 10000*g* for 10 min at 4 °C. The mitochondrial pellet was resuspended in 50 µl of homogenization buffer without EGTA and bovine serum albumin. The final supernatant was designated as the "cytosolic/membranes fraction" and was used to measure NADPH and xanthine oxidase activities. "Cytosolic/membranes fractions" from livers and kidneys were prepared according to the same protocol.

For Western blot experiments, mitochondria were purified on a Percoll® gradient [7,11]. The submitochondrial localization of the translocator protein (TSPO) was determined by use of a digitonin solubilization method to separate the outer mitochondrial membranes from the mitoplats as described previously [12]. Freshly prepared purified mitochondria were incubated in the presence of digitonin (0.8 mg/mg protein) for 15 min. At the end of this incubation period, the suspension was centrifuged for 10 min at 15000 g. The pellet was resuspended in the following buffer: 220 mM mannitol, 70 mM sucrose, 10 mM Hepes, 0.1 mM EGTA, pH 7.4 at 4 °C and designated the "mitoplasts". The supernatant contained the outer mitochondrial membranes released by the digitonin treatment.

2.3. Determination of mitochondrial reactive oxygen species production

Mitochondrial ROS generation was assessed by measuring the rate of hydrogen peroxide (H_2O_2) production through oxidation of Amplex red to fluorescent resorufin, coupled to the enzymatic reduction of

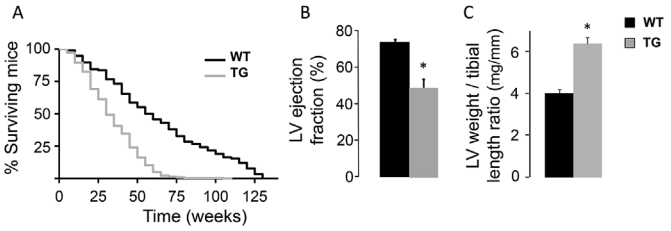

Fig. 1. Hsp22 overexpression reduces lifespan, left ventricular ejection and increases cardiac hypertrophy. A: Kaplan-Meier survival curve comparing WT and TG mice (WT mice: n = 116 and TG mice: n = 217). Mean life spans: 34.3 ± 1.18 and 63.3 ± 3.34 weeks for TG and WT mice, respectively ($p < 0.05$). B:LV ejection fraction was reduced in TG mice as compared to WT ($p < 0.05$). Each value represents the mean ± sem of five animals. *$p < 0.05$ *vs* WT. C: Increase in left ventricular (LV) weight to tibial length ratio as an index of left ventricular hypertrophy in control WT and TG mice ($p < 0.05$). Each value represents the mean ± sem of at least 11 animals. *$p < 0.05$ *vs* WT.

H_2O_2 by horseradish peroxidase as described previously [13]. Superoxide anion generated in mitochondria was converted endogenously to H_2O_2 and then measured by the assay. Briefly, amplex red (10 µM) and horseradish peroxidase (1 U/ml) were added to isolated mitochondria (0.2 mg protein) in a respiration buffer containing 100 mM KCl, 50 mM sucrose, 10 mM HEPES, 5 mM KH_2PO_4, pH 7.4 at 30 °C. The reaction was initiated by addition of the respiratory substrates (pyruvate/malate 5/5 mM or succinate 5 mM + rotenone 2 µM). The subsequent increase in fluorescence was monitored over time using a fluorescence spectrometer (Perkin-Elmer SA LS 50B, excitation wavelength 563 nm; emission wavelength 587 nm).

2.4. Western blot analysis

Proteins were denatured by boiling, resolved on SDS-PAGE 10% polyacrylamide gels, and transferred to polyvinylidenedifluoride membranes. Membranes were blocked with 5% nonfat dry milk in a Tris buffer (Tris 10 mM, NaCl 100 mM, pH 7.5) containing 0.1%Tween 20 for 1 h at room temperature. Subsequently, membranes were exposed for 12 h at 4 °C to either anti-Nox2/gp91phox (1:2000; Abcam), anti-Akt (1:2000; Cell Signaling), anti-pAkt (Ser 473, 1:2000; Cell Signaling), anti-Hsp22 (1:500 Abcam), anti-TSPO (1:2000; Abcam), anti-Voltage Dependent Anion Channel (VDAC, 1:2000; Cell Signaling) or anti-actin (1:2000; Cell Signaling). After incubation with goat anti-mouse (Santa Cruz Biotechnology) or goat anti-rabbit (Cell Signaling) as a secondary antibody at 1:5000, blots were revealed by *Pierce ECL Western Blotting Substrate* (Thermo Scientific) in a G:BOX chemi XT4 (Syngene). Bands were analyzed by densitometry with Genesys software (Syngene).

2.5. Quantitative RT-PCR

LV tissues were sampled from TG and WT mice. Total RNA was isolated from mouse LV tissues using the RNeasy Fibrous Tissue Mini Kit (Qiagen, Courtaboeuf, France). cDNA was synthesized from 1 µg of total RNA using the SuperScript first-strand synthesis system for the RT-PCR kit (Invitrogen, CergyPontoise, France) and random oligonucleotides. Expression of genes encoding p53, p16, p21, p19 was monitored by a real-time qRT-PCR method using an Applied Biosystems 7000 real-time PCR system. The ubiquitous 18S RNA was used to normalize the data across samples. Its expression was monitored by SYBRGreen incorporation.

2.6. Telomere length

After genomic DNA extraction using DNA Isolation Kit for Cells and

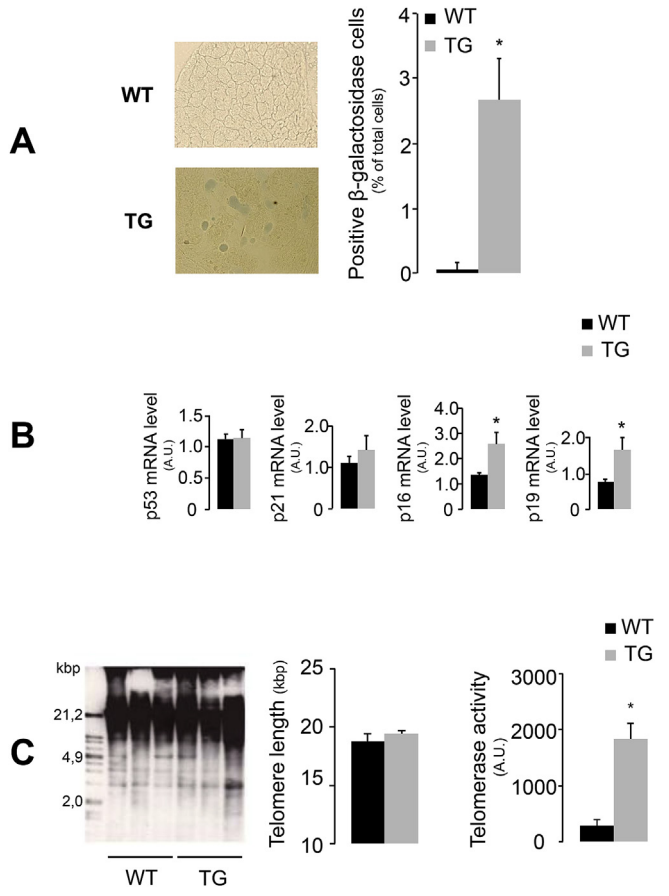

Fig. 2. Myocardial Hsp22 overexpression induces myocardial cellular senescence. A: Senescence determined by measurement of β-galactosidase positive cells (blue coloration) in the left ventricle from WT and TG mice. Left: Pictures from the subendocardial regions showed a positive β-galactosidase staining in TG mice which is absent in WT mice. Right: Percentage of β-galactosidase positive cells in hearts from WT and TG mice. Each value represents the mean ± sem of at least six hearts. *p < 0.05 *vs* WT. B: Myocardial mRNA levels of p53, p21, p16 and p19 were determined using quantitative RT-PCR in WT and TG mice. *p < 0.05 *vs* WT. A.U.:arbitrary unit. Each experiment was performed in duplicate on at least four animals. C: Telomere length was measured by southern blot after DNA digestion in hearts from WT and TG mice and telomerase activity was determined in cardiac homogenates from WT and TG mice. Each value represents the mean ± sem of at least six independent preparations. *p < 0.05 *vs* WT. A.U.: arbitrary unit. (For interpretation of the references to color in this figure legend, the reader is referred to the Web version of this article.)

Tissues (Roche), the measurement of telomere length was carried out with the TeloTAGGG Telomere Lenght Assay kit (Roche, Meylan, France) in accordance with the manufacturer's instructions. Briefly, DNA was digested with specific enzymes and then DNA fragments were separated by electrophoresis and transferred by Southern blot. DNA was detected by hybridizing a specific digoxigenin-coupled probe and anti-digoxigenin antibody coupled with alcalin phosphatase that had allowed chemiluminescent detection. Densitometry measure was used to determined telomere length.

2.7. Telomerase activity

Telomerase activity was analyzed with a *TeloTAGGG Telomerase PCR ELISA*^{PLUS}kit (Roche diagnostic, Manheim, Germany), in accordance with the manufacturer's instructions. This was assessed in 3 successive steps: 1) protein extraction and dosage, 2) elongation/amplification and 3) detection with an enzyme-linked immunosorbent assay. The absorbance was measured at 450 nm and telomerase activity calculated.

2.8. β-galactosidase staining

Left ventricle slices were fixed with 2% formaldehyde and 0.2% glutaraldehyde for 15 min at room temperature. Then, slices were washed with phosphate buffer saline and stained in a titrated pH 6 solution containing 40 mM citric acid, 150 mM NaCl, 2 mM MgCl2, 5 mM potassium ferrocyanide, and 1 mg/mL 5-bromo-4-chloro-3-indolyl-beta-D-galactoside (X-Gal; QIAGEN, courtabeuf, France). The slices were then immersed in a 4% formaldehyde solution which fixes the staining obtained.

2.9. GSH/GSSG ratio

Samples (10 mg) of left cardiac ventricle, liver or kidney were homogenized in 1 ml of sulfosalicylic acid (2%) by means of an Ultra Turrax homogenizer. The homogenate was centrifuged at 10000 g for 5 min and the supernatant was separated in two parts to measure total and oxidized (GSSG) glutathione levels. GSSG and reduced glutathione (GSH) levels were determined using the enzymatic recycling method [14].

2.10. Enzymatic assays

NADPH oxidase activity was measured in cytosolic/membrane fractions from WT and TG mice as the apocynin inhibitable superoxide anion production induced by NADPH. Superoxide anion production was evaluated with nitrobluetetrazolium which is reduced by superoxide anion in formazan. Samples (1 mg/mL) were introduced in a phosphate buffer saline maintained at 30 °C in the presence of NADPH (20 mM) and the appearance of formazan was followed spectrophotometrically (560 nm). Apocynin (1 mM) was added to evaluate specific NADPH oxidase formation of superoxide anion.

Xanthine oxidase activity was measured in the same cardiac fractions by monitoring the increase in absorbance resulting from the appearance of uric acid produced by xanthine oxidase. Samples (2 mg/mL) were introduced in a phosphate buffer saline maintained at 30 °C. The reaction was initiated by addition of xanthine (100 µM) and uric acid production was followed spectrophotometrically (290 nm). A blank was obtained in the same conditions but in absence of xanthine.

2.11. Determination of mitochondrial cholesterol and oxysterol levels

Mitochondria (5 mg protein/ml) were added to a chloroform-Triton X-100 1% mixture (v:v) and submitted to strong agitation for 1 min. The samples were centrifuged at 8,000 g for 5 min at room temperature. The upper phases were discarded and the lower phases containing cholesterol and sterols in the presence of deuterium labeled internal standards underwent an alkaline hydrolysis with ethanolic KOH, separation by liquid to liquid extraction, evaporation under nitrogen stream and derivatisation with BSTFA-TMS 1% for 1 h at 60 °C. Cholesterol and oxysterols were assayed in mitochondria extracts by isotope dilution-mass spectrometry as described previously [15].

2.12. Statistical analysis

Results are presented as the mean ± sem for the number of samples indicated in the legends. Statistical comparison was performed using the Student t-test. Two-way analysis of variance followed by Scheffe's post-test was used for multi-group comparison. The statistics for survival was determined by the Log-Rank Test. Statistical significance was set at $p < 0.05$.

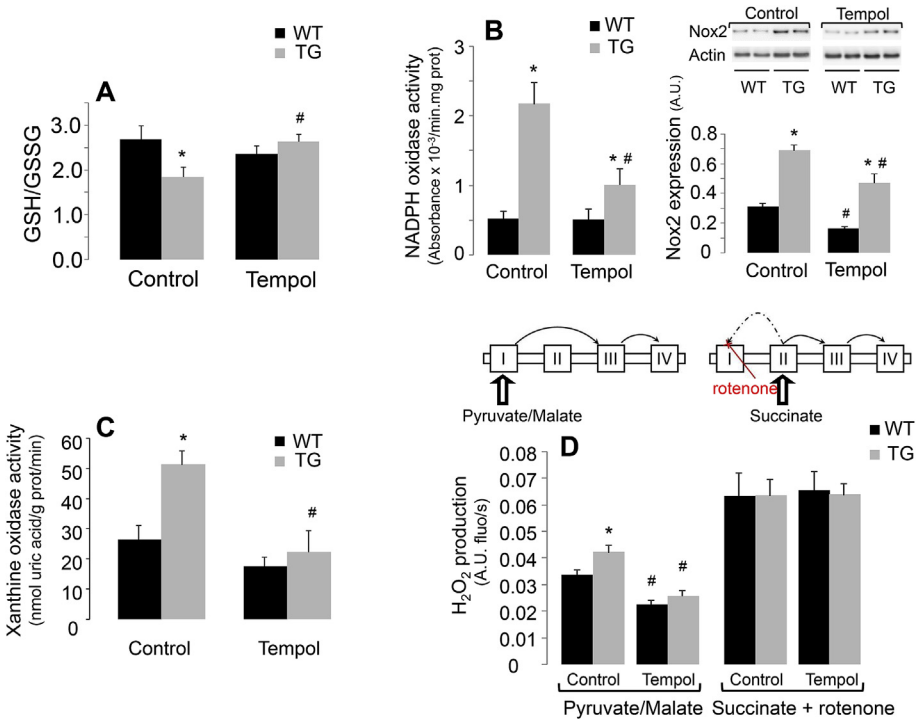

Fig. 3. Hsp22 overexpression enhances ROS production and oxidative stress in transgenic mice and these effects are abolished by Tempol treatment. Mice were treated with Tempol (100 mg/kg/day) or vehicle (control) from their weaning to their sacrifice. A: GSH and GSSG contents were determined spectrophotometrically (412 nm) with 5,5′-Dithiobis-(2-Nitrobenzoic Acid) in cardiac homogenates from control and treated WT and TG mice and GSH/GSSG *ratio* was calculated. Each value represents the mean ± sem of preparations from at least six animals. *p < 0.05 *vs* WT. #p < 0.05 *vs* respective control. B: NADPH oxidase activity was evaluated in cardiac homogenates from control and treated WT and TG mice. Nox-2 expression was measured in cardiac homogenates from control and treated WT and TG mice by Western blot and was quantified relative to actin. Each value represents the mean ± sem of preparations from at least six animals. *p < 0.05 *vs* WT. #p < 0.05 *vs* respective control. C: Xanthine oxidase activity was assessed by measuring the appearance of uric acid (290 nm) in cardiac homogenates from control and treated WT and TG mice. Each value represents the mean ± sem of preparations from at least six animals. *p < 0.05 *vs* WT. #p < 0.05 *vs* respective control. D: H_2O_2 production was induced by pyruvate/malate (5/5 mM) or succinate (5 mM) in the presence of rotenone (2 μM) and was determined fluorometrically by the oxidation of Amplex red to fluorescent resorufin in isolated mitochondria from control and treated WT and TG mice. Each value represents the mean ± sem of preparations from at least eight animals. *p < 0.05 *vs* WT. #p < 0.05 *vs* respective control. A.U. (fluo): arbitrary units (of fluorescence). (For interpretation of the references to color in this figure legend, the reader is referred to the Web version of this article.)

3. Results

3.1. Myocardial Hsp22 overexpression reduced life span and was associated with senescence markers in mice

To assess the effect of myocardial Hsp22 overexpression on longevity, we examined the life span of WT and TG mice (Fig. 1A). Life span of TG mice was shortened as compared to WT with TG mice dying at a faster rate (Fig. 1A). The life span of TG mice did not exceed 60 weeks whereas 30% of WT mice stayed alive at this age. The mean life span was 34.3 ± 1.2 and 63.3 ± 3.3 weeks for TG and WT mice, respectively. This reduction of life span in TG mice was associated with a reduction of left ventricular (LV) ejection fraction in one year old TG mice (49% vs 74% in WT, p < 0.01; Fig. 1B) and significant LV hypertrophy which was already observed in 10–12 week old mice, as shown by the significant increase in LV/tibial length ratio (4.0 ± 0.1 *vs* 6.3 ± 0.2 mg/mm in WT *vs* TG mice, respectively (n = 13); Fig. 1C).

At the cellular level, hearts from TG mice displayed ß-galactosidase positive cells, a well-known marker of senescence. This marker was already present in the myocardium of young adult TG mice (10–12 week old) whereas it was not detectable in WT mice of the same age (Fig. 2A). At the molecular level, senescent cells were characterized by an overexpression of cell cycle inhibiting proteins [16]. We observed that the cell cycle inhibitors p16 and p19 increased in the myocardium of young adult TG mice compared to WT mice, whereas expression of the transcription factor p53 and cyclin-dependent kinase inhibitor p21 were not modified (Fig. 2B). The enhancement of p16 and p19 was rather specific to the myocardium as it was not found in the kidney (Fig. S1), confirming that the effect was related to Hsp22 overexpression. A typical feature of senescent cells is a decrease in telomere length. To confirm the senescent profile of the myocardium of TG mice, we compared the telomere length of the genomic DNA extracted from WT and TG mice. As shown in Fig. 2C, we did not observe any significant variation in the length of telomeres between WT and TG mice. This could be due to the fact that the telomeres of the murine DNA are large, which makes it very difficult to detect the reduction of their size. Fig. 2C also shows that myocardium from TG mice displayed a very high activity of telomerase as compared to WT mice.

3.2. Myocardial Hsp22 overexpression induced cardiac oxidative stress

To evaluate oxidative stress, we measured the concentrations of reduced GSH and GSSG in whole myocardial homogenates of 10–12 week old mice. While concentrations of GSH were unchanged in TG compared to WT mice (804 ± 46 and 894 ± 89 nmol/g tissue in WT and TG mice, respectively), the amount of GSSG increased in TG mice (489 ± 17 nmol/g tissue) compared to WT mice (307 ± 17 nmol/g tissue; p < 0.05). This resulted in a lower GSH/GSSG ratio in TG mice (Fig. 3A). Several sources of ROS are responsible for the enhancement of oxidative stress in TG mice. The first one is NADPH oxidase which is a major generator of ROS production in the cardiovascular system [17]. The activity of the enzyme was strongly stimulated in TG mice (Fig. 3B) and this can be ascribed to an increase in the expression of the protein as demonstrated by immunoblotting of Nox2 (Fig. 3B). Similarly, the activity of xanthine oxidase, which produces hydrogen peroxide in the cell, was more important in TG than in WT mice (Fig. 3C). Such changes were selective to the myocardium as the significant increases in activities of NADPH and xanthine oxidase as well as GSSG/GSH ratio were not observed in other organs of TG mice (Fig. S2). The mitochondrial respiratory chain also contributes to the oxidative stress. Indeed, Fig. 3D confirms our results demonstrating that Hsp22 overexpression increases the net production of H_2O_2 from mitochondria in the basal state. This effect was related to the activation of complex I [7] as ROS production increased when the respiratory chain was fed with pyruvate/malate but not with succinate in the presence of rotenone.

The translocator protein TSPO, another mitochondrial component emerging as a modulator of oxidative stress [18,19], has been shown to interact with the voltage-dependent anion channel (VDAC) and to promote ROS production [20]. In an attempt to better understand the mechanisms of the increased ROS production, we therefore measured

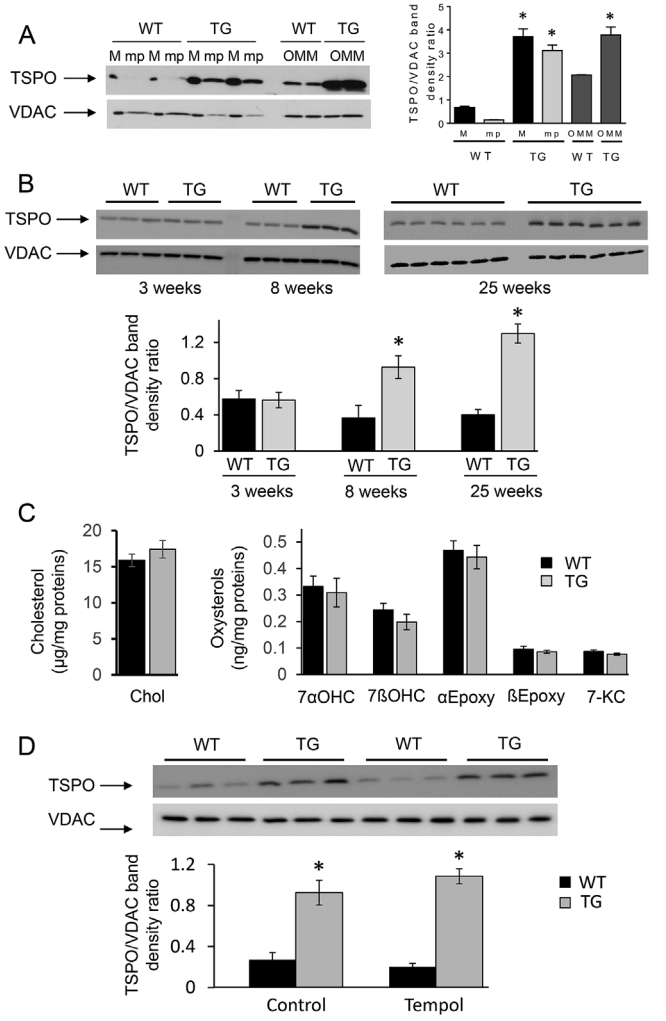

Fig. 4. Hsp22 overexpression enhances TSPO expression in cardiac mitochondria. A: Western Blot experiments of the expression of TSPO in mitochondria (M), mitoplasts (mp) and outer mitochondrial membranes (OMM) in WT and TG mice of 8 week old. B: Western blot experiments and band density analysis showing the increase in the mitochondrial TSPO/VDAC ratio during ageing in TG mice. C: Cholesterol and oxysterol levels were not altered in cardiac mitochondria isolated from TG mice. Each value represents the mean ± sem of 8 independent preparations. Chl: cholesterol; 7αOHC: 7α-hydroxycholesterol; 7βOHC: 7β-hydroxycholesterol; 7 KC: 7-ketocholesterol; αEpoxy: cholesterol-5α,6α-epoxide; βEpoxy: cholesterol-5β,6β-epoxide. D: Western blot experiments and band density analysis showing the increase in the mitochondrial TSPO/VDAC ratio in cardiac mitochondria from control and Tempol treated WT and TG mice of 8 week old. Each value represents the mean ± sem of at least three independent preparations. *p < 0.05 *vs* WT.

the expression of TSPO in mitochondria issued from WT and TG mice. First, the expression was evaluated on purified mitochondria, mitoplasts and mitochondrial outer membranes. Immunoblotting analysis confirmed the presence of TSPO in the outer membrane of cardiac mitochondria and showed that TSPO expression was higher in 8 week old TG mice compared to WT mice (Fig. 4A). As shown in Fig. 4B, the ratio TSPO/VDAC remained similar in mitochondria issued from young mice (3 weeks) and then increased with age. As TSPO is considered as one of the proteins that facilitates the transport of cholesterol into mitochondria [21], we determined whether the overexpression of TSPO was associated with an accumulation of cholesterol and a subsequent increase in its oxidative derivatives oxysterols in cardiac TG mitochondria. As shown in Fig. 4C, the concentration of cholesterol and oxysterols remained similar in cardiac mitochondria of TG and WT mice.

3.3. Tempol reduced oxidative stress in TG mice

To clarify the potential role of the observed oxidative stress in the phenotype of TG mice, mice were treated from the weaning to the adulthood with Tempol (100 mg/kg/day), a membrane permeable and general antioxidant, that was shown to reduce the markers of oxidative stress in membrane, cytosol and mitochondrial compartments [22,23]. First, we verified that Tempol did not modify the expression of Hsp22 in 10–12 week old TG mice (Fig. S3). Then, we observed that Tempol had no effect on GSH and GSSG contents in WT mice but in TG mice, GSH was increased (from 895 ± 89 in control to 1124 ± 52 in treated TG mice; $p < 0.05$) and GSSG was decreased (from 489 ± 17 in control to 427 ± 6 in treated TG mice; $p < 0.05$). In these conditions, Tempol abolished the difference in GSH/GSSG ratio previously observed between WT and TG mice (Fig. 3A). This effect can be accounted for by the significant decrease in ROS production induced by NADPH (Fig. 3B), xanthine oxidase (Fig. 3C) and by the mitochondrial respiratory chain (Fig. 3D). As shown in Fig. 4D, this effect was not related to a decrease in TSPO/VDAC ratio which was not modified by Tempol.

3.4. Tempol treatment reduced myocardial hypertrophy and senescence markers and improved lifespan in mice

As oxidative stress and ROS generated by NADPH oxidase play a key role in myocardial hypertrophy [8], we investigated the effect of Tempol treatment on this parameter in 10–12 week old TG mice. Myocardial hypertrophy was significantly reduced in TG mice receiving Tempol, underlying for the first time the role of oxidative stress in this model (Fig. 5A) and no effect was observed in WT mice. Previous studies highlighted an increase in Akt phosphorylation in the hypertrophic effect mediated by Hsp22 [1,2]. Here, Tempol significantly blunted the increase in pAkt/Akt ratio (Fig. 5B).

Concomitantly, Tempol also lowered the aging markers that were shown to be increased in TG mice. Fig. 5C shows that both p16 and p19 mRNA levels were reduced in TG mice after Tempol treatment, reaching the levels found in WT mice. This was associated with an abolition of the increased mortality caused by Hsp22 overexpression at 30 weeks, the life span of treated TG mice being similar to that of WT mice (Fig. 5D). This result demonstrates that oxidative stress is the mediator by which Hsp22 over-expression induces over-mortality in mice and importantly that this effect can be reversed by an antioxidant treatment.

4. Discussion

The present study demonstrates that Hsp22 overexpression leads to senescence, reduced lifespan and cardiac hypertrophy due to a significant augmentation of oxidative stress mediated by enhanced activities of major sources of ROS production, *i.e.*, the mitochondrial respiratory chain, NADPH and xanthine oxidase. TSPO may also contribute to the oxidative stress. Indeed, Hsp22 overexpression enhanced TSPO expression, a property that has been shown to increase the accumulation of ROS, to limit the efficiency of mitochondrial autophagy [20] suggesting that it participates in the hypertrophic response observed in TG mice [24]. The overexpression of TSPO could be linked to the Hsp22-dependent activation of the PKCε and STAT3 pathways [6,25] which have been described to drive *tspo* transcription and protein expression [26]. This increase in TSPO/VDAC ratio does not seem to be a consequence, but rather a contributor to the oxidative stress, as it was not modified by the Tempol treatment. Finally, the contribution of TSPO on oxidative stress is not related to its well-known role in cholesterol transport [21] as mitochondrial cholesterol and oxysterol accumulation was not altered in TG mice.

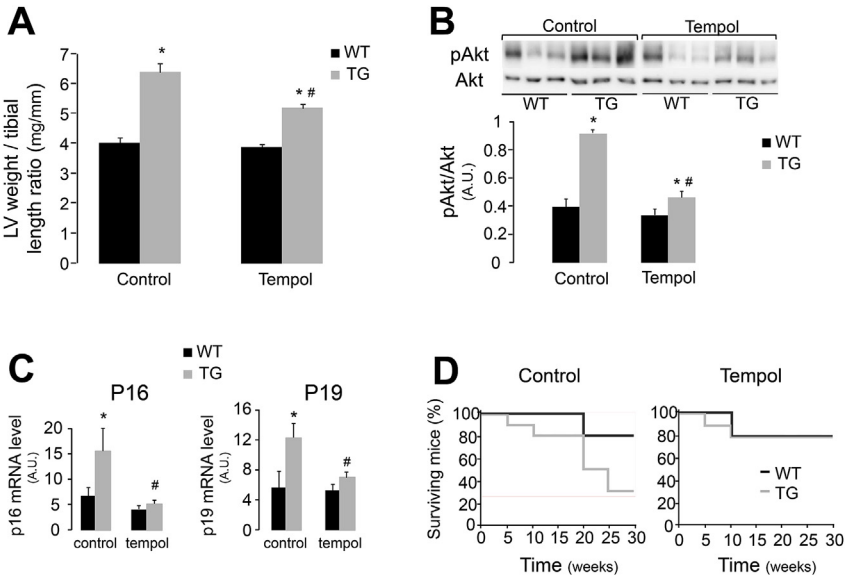

Fig. 5. Tempol treatment reduces myocardial hypertrophy and senescence markers and improves lifespan in Hsp22 overexpressing mice. Mice were treated with Tempol (100 mg/kg/day) or vehicle (control) from their weaning to their sacrifice. A: Left ventricular (LV) weight over tibial length ratio in control and treated WT and TG mice. Each value represents the mean ± sem of at least 11 animals. *p < 0.05 *vs* WT; #p < 0.05 *vs* respective control. B: pAkt protein level was measured by Western blot in cardiac homogenates from control and treated WT and TG mice and quantified relative to Akt. Pictures were quantified and each value represents the mean ± sem of at least six independent preparations. *p < 0.05 *vs* WT; #p < 0.05 *vs* respective control. A.U.: arbitrary unit. C: Myocardial mRNA levels of p16 and p19 were determined using quantitative RT-PCR in control and treated WT and TG mice. *p < 0.05 *vs* WT. #p < 0.05 *vs* respective control. A.U.: arbitrary unit. D: Mice were treated with Tempol (100 mg/kg/day) or vehicle from the weaning and during 7 months and survival curves for control and treated WT and TG mice were plotted (n = 10 per group).

Our data demonstrate that this oxidative stress participates in the activation of signaling pathways involved in growth. Indeed, the treatment of TG mice with the general antioxidant Tempol strongly inhibited ROS production and limited the development of myocardial hypertrophy underlying the role of oxidative stress in this model. As Tempol treatment only began just after weaning (3–4 weeks) when hypertrophy was already established [4], it should be emphasized that ROS inhibition prevented the progression of LV hypertrophy but did not reverse a process which was already in place. A growing body of evidence reveals the causative role of redox-sensitive pathways in the processes underlying cardiac hypertrophy [8] and the antihypertrophic effect of Tempol was previously described in various models of myocardial hypertrophy. For example, Tempol was shown to reduce myocardial hypertrophy in insulin resistant GLUT4-knockout mice [10] and to prevent this process in a model of aortic banding [27]. Numerous studies have suggested a key role of ROS generated by NADPH oxidase in cardiac hypertrophy. Interestingly, the expression and activity of this enzyme were increased in TG mice and these effects were also reduced by Tempol. One of the signaling pathways involved in this hypertrophic effect related to NADPH oxidase is the Akt pathway, which is also one of the main pathways implicated in Hsp22-induced hypertrophy [1]. The present study shows that the activation of Akt by Hsp22 is inhibited by Tempol and therefore is the consequence of ROS overproduction. Taken together these data support the concept that Hsp22 overexpression is responsible for the activation of a global ROS production which stimulates the Akt pathway and consequently hypertrophy. However, it should be acknowledged that other mechanisms could participate to the development of LV hypertrophy. For example, proteasome activation has been shown to be involved in Hsp22-induced hypertrophy [4].

Our study further demonstrates that, the oxidative stress promoted by Hsp22 overexpression induces senescence and reduced lifespan. Multiple mechanisms such as suppression of the growth hormone/insulin-like growth factor axis [28,29], deletion of p66shc adaptator protein [30] or disruption of type 5 adenylyl cyclase [31] have been involved in the regulation of lifespan. They are associated to increasing resistance to oxidative stress which plays a determinant role to extend life span [32,33]. Indeed, it is well established that aging and lifespan are correlated with oxidative stress [34–36]. Excessive ROS production and oxidative stress damages the structure of DNA, phospholipids, and proteins, resulting in cellular and tissue injury. This is a critical mechanism for ROS-induced aging [37]. Hearts from TG mice produced high levels of ROS and showed a significant increase in β-galactosidase positive cells as well as p16 and p19 mRNA levels, which are key characteristics of senescence and have been shown to be increased in several cardiac cell lines during aging [38–41]. These findings characterize a premature aging rather than a replicative senescence process induced by telomere erosion. This supports the hypothesis that the elevated oxidative stress is also involved in these pathophysiological responses observed in TG mice. This is confirmed by the fact that Tempol treatment prevents the increase in p16 and p19 mRNA levels. Interestingly, Hsp22-overexpression was also associated with a high telomerase activity which is usually very low in quiescent tissues such as the heart. This can also participate in the premature senescence as high telomerase activity can promote a senescence phenotype [42]. Cellular senescence is often accompagnied by a senescence-associated secretory phenotype (SASP) which is characterized by the secretion of bioactive molecules such as cytokines, proteases or regulatory factors [43]. SASP can lead to tissue dysfunction and has been involved in the development of cardiac hypertrophy [44,45] and it would be interesting to assess the potential role of SASP in the development of left ventricle hypertrophy by Hsp22 overexpression.

Paradoxically, Hsp22 overexpression in *Drosophila* has been associated with increased resistance against oxidative stress and prolonged life span [5]. This opposite behavior may likely be explained by the location of Hsp22 which is only in the mitochondria in *Drosophila*. It is conceivable that a cytosolic source of ROS may be necessary to develop a senescent phenotype in Hsp22 overexpressing mice. However, it is still unknown how expression of Hsp22 increases the activity of the protein producing ROS and this is a limitation of the study. Further investigations are needed to determine this mechanism.

In conclusion, Hsp22 overexpression increases oxidative stress, which results in the induction of hypertrophy and senescence and ultimately reduction in life span.

Sources of funding

R. Long was supported by a doctoral grant from the Ministère de la Recherche et de la Technologie.

Disclosures

Nothing to declare.

Appendix A. Supplementary data

Supplementary data to this article can be found online at https://doi.org/10.1016/j.freeradbiomed.2019.04.035.

References

[1] J. Acunzo, M. Katsogiannou, P. Rocchi, Small heat shock proteins HSP27 (HspB1), αB-crystallin (HspB5) and HSP22 (HspB8) as regulators of cell death, Int. J. Biochem. Cell Biol. 4 (2012) 1622–1631, https://doi.org/10.1016/j.biocel.2012.04.002.

[2] C. Depre, M. Hase, V. Gaussin, A. Zajac, L. Wang, L. Hittinger, B. Ghaleb, X. Yu, R.K. Kudej, T. Wagner, J. Sadoshima, S.F. Vatner, H11 Kinase is a novel mediator of myocardial hypertrophy in vivo, Circ. Res. 91 (2002) 1007–1014.

[3] C. Depre, S.J. Kim, A.S. John, Y. Huang, O.E. Rimoldi, J.R. Pepper, G.D. Dreyfus, V. Gaussin, D.J. Pennell, D.E. Vatner, P.G. Camici, S.F. Vatner, Program of cell survival underlying human and experimental hibernating myocardium, Circ. Res. 95 (2004) 433–440, https://doi.org/10.1161/01.RES.0000138301.42713.18.

[4] N. Hedhli, L. Wang, Q. Wang, E. Rashed, Y. Tian, X. Sui, K. Madura, C. Depre, Proteasome activation during cardiac hypertrophy by the chaperone H11 Kinase/Hsp22, Cardiovasc. Res. 77 (2008) 497–505, https://doi.org/10.1093/cvr/cvm054.

[5] G. Morrow, S. Battistini, P. Zhang, R.M. Tanguay, Decreased lifespan in the absence of expression of the mitochondrial small heat shock protein Hsp22 in Drosophila, J. Biol. Chem. 279 (2004) 43382–43385, https://doi.org/10.1074/jbc.C400357200.

[6] H. Qiu, P. Lizano, L. Laure, X. Sui, E. Rashed, J.Y. Park, C. Hong, S. Gao, E. Holle, D. Morin, S.K. Dhar, T. Wagner, A. Berdeaux, B. Tian, S.F. Vatner, C. Depre, H11 kinase/heat shock protein 22 deletion impairs both nuclear and mitochondrial functions of STAT3 and accelerates the transition into heart failure on cardiac overload, Circulation 124 (2011) 406–415, https://doi.org/10.1161/CIRCULATIONAHA.110.013847.

[7] L. Laure, R. Long, P. Lizano, R. Zini, A. Berdeaux, C. Depre, D. Morin, Cardiac H11 kinase/Hsp22 stimulates oxidative phosphorylation and modulates mitochondrial reactive oxygen species production: involvement of a nitric oxide-dependent mechanism, Free Radic. Biol. Med. 52 (2012) 2168–2176, https://doi.org/10.1016/j.freeradbiomed.2012.03.001.

[8] S.K. Maulik, S. Kumar, Oxidative stress and cardiac hypertrophy: a review, Toxicol. Mech. Methods 22 (2012) 359–366, https://doi.org/10.3109/15376516.2012.666650.

[9] M. Gilca, I. Stoian, V. Atanasiu, B. Virgolici, The oxidative hypothesis of senescence, J. Postgrad. Med. 53 (2007) 207–213.

[10] R.H. Ritchie, J.M. Quinn, A.H. Cao, G.R. Drummond, D.M. Kaye, J.M. Favaloro, J. Proietto, L.M. Delbridge, The antioxidant tempol inhibits cardiac hypertrophy in the insulin-resistant GLUT4-deficient mouse in vivo, J. Mol. Cell. Cardiol. 42 (2007) 1119–1128, https://doi.org/10.1016/j.yjmcc.2007.03.900.

[11] P.A. Townsend, S.M. Davidson, S.J. Clarke, I. Khaliulin, C.J. Carroll, T.M. Scarabelli, R.A. Knight, A. Stephanou, D.S. Latchman, A.P. Halestrap, Urocortin prevents mitochondrial permeability transition in response to reperfusion injury indirectly by reducing oxidative stress, Am. J. Physiol. Heart Circ. Physiol. 293 (2007) H928–H938, https://doi.org/10.1152/ajpheart.01135.2006.

[12] R.R. Anholt, P.L. Pedersen, E.B. De Souza, S.H. Snyder, The peripheral-type benzodiazepine receptor. Localization to the mitochondrial outer membrane, J. Biol. Chem. 261 (1986) 576–583.

[13] L. Lo Iacono, J. Boczkowski, R. Zini, I. Salouage, A. Berdeaux, R. Motterlini, D. Morin, A carbon monoxide-releasing molecule (CORM-3) uncouples mitochondrial respiration and modulates the production of reactive oxygen species, Free Radic. Biol. Med. 50 (2011) 1556–1564, https://doi.org/10.1016/j.freeradbiomed.2011.02.033.

[14] I. Rahman, A. Kode, S.K. Biswas, Assay for quantitative determination of glutathione and glutathione disulfide levels using enzymatic recycling method, Nat. Protoc. 1 (2006) 3159–3165, https://doi.org/10.1038/nprot.2006.378.

[15] V. Leoni, L. Strittmatter, G. Zorzi, F. Zibordi, S. Dusi, B. Garavaglia, P. Venco, C. Caccia, A.L. Souza, A. Deik, C.B. Clish, M. Rimoldi, E. Ciusani, E. Bertini, N. Nardocci, V.K. Mootha, V. Tiranti, Metabolic consequences of mitochondrial coenzyme A deficiency in patients with PANK2 mutations, Mol. Genet. Metabol. 105 (2012) 463–471, https://doi.org/10.1016/j.ymgme.2011.12.005.

[16] F. Bringold, M. Serrano, Tumor suppressors and oncogenes in cellular senescence, Exp. Gerontol. 35 (2000) 317–329.

[17] K.K. Griendling, D. Sorescu, M. Ushio-Fukai, NAD(P)H oxidase: role in cardiovascular biology and disease, Circ. Res. 86 (2000) 494–501.

[18] H. Batoko, V. Veljanovski, P. Jurkiewicz, Enigmatic Translocator protein (TSPO) and cellular stress regulation, Trends Biochem. Sci. 40 (2015) 497–503, https://doi.org/10.1016/j.tibs.2015.07.001.

[19] D. Morin, J. Musman, S. Pons, A. Berdeaux, B. Ghaleb, Mitochondrial translocator protein (TSPO): from physiology to cardioprotection, Biochem. Pharmacol. 105 (2016) 1–13, https://doi.org/10.1016/j.bcp.2015.12.003.

[20] J. Gatliff, D. East, J. Crosby, R. Abeti, R. Harvey, W. Craigen, P. Parker, M. Campanella, TSPO interacts with VDAC1 and triggers a ROS-mediated inhibition of mitochondrial quality control, Autophagy 10 (2014) 2279–2296, https://doi.org/10.4161/15548627.2014.991665.

[21] V. Papadopoulos, Y. Aghazadeh, J. Fan, E. Campioli, B. Zirkin, A. Midzak, Translocator protein-mediated pharmacology of cholesterol transport and steroidogenesis, Mol. Cell. Endocrinol. 408 (2015) 90–98, https://doi.org/10.1016/j.mce.2015.03.014.

[22] S. Kimura, G.X. Zhang, A. Nishiyama, T. Shokoji, L. Yao, Y.Y. Fan, M. Rahman, T. Suzuki, H. Maeta, Y. Abe, Role of NAD(P)H oxidase- and mitochondria-derived reactive oxygen species in cardioprotection of ischemic reperfusion injury by angiotensin II, Hypertension 45 (2005) 860–866, https://doi.org/10.1161/01.HYP.0000163462.98381.7f.

[23] N. Mariappan, R.N. Soorappan, M. Haque, S. Sriramula, J. Francis, TNF-alpha-induced mitochondrial oxidative stress and cardiac dysfunction: restoration by superoxide dismutase mimetic tempol, Am. J. Physiol. Heart Circ. Physiol. 293 (2007) H2726–H2737, https://doi.org/10.1152/ajpheart.00376.2007.

[24] K. Nishida, K. Otsu, Autophagy during cardiac remodeling, J. Mol. Cell. Cardiol. 95 (2016) 11–18, https://doi.org/10.1016/j.yjmcc.2015.12.003.

[25] I.J. Danan, E.R. Rashed, C. Depre, Therapeutic potential of H11 kinase for the ischemic heart, Cardiovasc. Drug Rev. 25 (2007) 14–29, https://doi.org/10.1111/j.1527-3466.2007.00002.x.

[26] A. Batarseh, J. Li, V. Papadopoulos, Protein kinase C epsilon regulation of translocator protein (18 kDa) Tspo gene expression is mediated through a MAPK pathway targeting STAT3 and c-Jun transcription factors, Biochemistry 49 (2010) 4766–4778, https://doi.org/10.1021/bi100020e.

[27] D.J. Chess, W. Xu, R. Khairallah, K.M. O'Shea, W.J. Kop, A.M. Azimzadeh, W.C. Stanley, The antioxidant tempol attenuates pressure overload-induced cardiac hypertrophy and contractile dysfunction in mice fed a high-fructose diet, Am. J. Physiol. Heart Circ. Physiol. 295 (2008) H2223–H2230, https://doi.org/10.1152/ajpheart.00563.2008.

[28] M. Holzenberger, J. Dupont, B. Ducos, P. Leneuve, A. Geloen, P.C. Even, P. Cervera, Y. Le Bouc, IGF-1 receptor regulates lifespan and resistance to oxidative stress in mice, Nature 421 (2003) 182–187, https://doi.org/10.1038/nature01298.

[29] Y.F. Chen, C.Y. Wu, C.H. Kao, T.F. Tsai, Longevity and lifespan control in mammals: lessons from the mouse, Ageing Res. Rev. 9 (2010) S28–S35, https://doi.org/10.1016/j.arr.2010.07.003.

[30] E. Migliaccio, M. Giorgio, S. Mele, G. Pelicci, P. Reboldi, P.P. Pandolfi, L. Lanfrancone, P.G. Pelicci, The p66shc adaptor protein controls oxidative stress response and life span in mammals, Nature 402 (1999) 309–313, https://doi.org/10.1038/46311.

[31] L. Yan, D.E. Vatner, J.P. O'Connor, A. Ivessa, H. Ge, W. Chen, S. Hirotani, Y. Ishikawa, J. Sadoshima, S.F. Vatner, Type 5 adenylyl cyclase disruption increases longevity and protects against stress, Cell 130 (2007) 247–258, https://doi.org/10.1016/j.cell.2007.05.038.

[32] R.S. Sohal, R. Weindruch, Oxidative stress, caloric restriction, and aging, Science 273 (1996) 59–63.

[33] S. Murakami, A. Salmon, R.A. Miller, Multiplex stress resistance in cells from long-lived dwarf mice, FASEB J. 17 (2003) 1565–1566, https://doi.org/10.1096/fj.02-1092fje.

[34] D. Harman, Aging: a theory based on free radical and radiation chemistry, J. Gerontol. 11 (1956) 298–300.

[35] G. Barja, The mitochondrial free radical theory of aging, Prog. Mol. Biol. Transl. Sci. 127 (2014) 1–27, https://doi.org/10.1016/B978-0-12-394625-6.00001-5.

[36] I. Liguori, G. Russo, F. Curcio, G. Bulli, L. Aran, D. Della-Morte, G. Gargiulo, G. Testa, F. Cacciatore, D. Bonaduce, P. Abete, Oxidative stress, aging, and diseases, Clin. Interv. Aging 13 (2018) 757–772, https://doi.org/10.2147/CIA.S158513.

[37] R.S. Sohal, W.C. Orr, The redox stress hypothesis of aging, Free Radic. Biol. Med. 52 (2012) 539–555, https://doi.org/10.1016/j.freeradbiomed.2011.10.445.

[38] C. Chimenti, J. Kajstura, D. Torella, K. Urbanek, H. Heleniak, C. Colussi, F. Di Meglio, B. Nadal-Ginard, A. Frustaci, A. Leri, A. Maseri, P. Anversa, Senescence and death of primitive cells and myocytes lead to premature cardiac aging and heart failure, Circ. Res. 93 (2003) 604–613, https://doi.org/10.1161/01.RES.0000093985.76901.AF.

[39] D. Torella, M. Rota, D. Nurzynska, E. Musso, A. Monsen, I. Shiraishi, E. Zias, K. Walsh, A. Rosenzweig, M.A. Sussman, K. Urbanek, B. Nadal-Ginard, J. Kajstura, P. Anversa, A. Leri, Cardiac stem cell and myocyte aging, heart failure, and insulin-like growth factor-1 overexpression, Circ. Res. 94 (2004) (28 2004) 514–524, https://doi.org/10.1161/01.RES.0000117306.10142.50.

[40] L.S. Wong, P. van der Harst, R.A. de Boer, J. Huzen, W.H. van Gilst, D.J. van Veldhuisen, Aging, telomeres and heart failure, Heart Fail. Rev. 15 (2010) 479–486, https://doi.org/10.1007/s10741-010-9173-7.

[41] H.J. De Jong, C.M. Woolthuis, E.S. de Bont, G. Huls, Paradoxial down-regulation of p16INK4a mRNA with advancing age in acute myeloid leukemia, Aging (N Y) 1 (2009) 949–953, https://doi.org/10.18632/aging.100096.

[42] V. Gorbunova, A. Seluanov, O.M. Pereira-Smith, Evidence that high telomerase activity may induce a senescent-like growth arrest in human fibroblasts, J. Biol. Chem. 278 (2003) 7692–7698, https://doi.org/10.1074/jbc.M212944200.

[43] M. Kumar, W. Seeger, R. Voswinckel, Senescence-associated secretory phenotype and its possible role in chronic obstructive pulmonary disease, Am. J. Respir. Cell Mol. Biol. 51 (2014) 323–333, https://doi.org/10.1165/rcmb.2013-0382PS.

[44] R. Anderson, A. Lagnado, D. Maggiorani, A. Walaszczyk, E. Dookun, J. Chapman, J. Birch, H. Salmonowicz, M. Ogrodnik, D. Jurk, C. Proctor, C. Correia-Melo, S. Victorelli, E. Fielder, R. Berlinguer-Palmini, A. Owens, L.C. Greaves, K.L. Kolsky, A. Parini, V. Douin-Echinard, N.K. LeBrasseur, H.M. Arthur, S. Tual-Chalot, M.J. Schafer, C.M. Roos, J.D. Miller, N. Robertson, J. Mann, P.D. Adams, T. Tchkonia, J.L. Kirkland, J. Mialet-Perez, G.D. Richardson, J.F. Passos, Length-independent telomere damage drives post-mitotic cardiomyocyte senescence, EMBO J. 38 (2019) e100492, , https://doi.org/10.15252/embj.2018100492.

[45] K. Shinmura, Cardiac senescence, heart failure, and frailty: a triangle in elderly people, Keio J. Med. 65 (2016) 25–32, https://doi.org/10.2302/kjm.2015-0015-IR.